Reduced-complexity spatial and temporal processing of underwater acoustic communication signals

M. Stojanovic, J. A. Catipovic,[a] and J. G. Proakis
Department of Electrical and Computer Engineering, Northeastern University, Boston, Massachusetts 02115

(Received 23 December 1993; accepted for publication 6 March 1995)

Multichannel processing of high-speed underwater acoustic communication signals requires computationally intensive receiver algorithms. The size of adaptive filters, determined by the extent of ocean multipath, increases with signaling rate and limits system performance through large noise enhancement and increased sensitivity of computationally efficient algorithms to numerical errors. To overcome these limitations, reduction in receiver complexity is achieved by exploiting the relationship between optimal diversity combining and beamforming. Under relatively simple conditions, two adaptive receivers, one based on diversity combining which does not rely on any spatial signal distribution, and the other based on optimal beamforming, are shown to achieve the same performance. The beamforming approach, however, leads to a receiver of lower complexity. Carrying these observations over to a general case of broadband transmission through an unknown channel, a fully adaptive receiver is developed which incorporates a multi-input multi-output, many-to-few combiner, and a reduced-complexity multichannel equalizer. Receiver operations are optimized jointly to ensure minimum mean-squared error performance of data detection. Results of processing experimental shallow water data demonstrate the capability to fully exploit spatial diversity of underwater multipath while keeping the complexity at an acceptable level. © *1995 Acoustical Society of America.*

PACS numbers: 43.60.Gk, 43.30.Wi

INTRODUCTION

A major problem for achieving reliable, high-speed underwater acoustic (UWA) communications is the large amount of intersymbol interference (ISI) encountered in many of the ocean channels. Examples of dynamic multipath ocean channels include mainly the horizontal channels, such as long-range deep water channels, in which many propagation paths meet at multiple convergence zones, and various shallow water channels in which multipath is comprised of both deterministic and random, bottom, volume and surface reverberation. Depending on the signaling rate used, ocean multipath can impose severe limitations on coherent reception, due to both its large time and frequency spreads.

Two basic strategies for dealing with multipath in UWA communications are (1) to design signals which ensures the absence of ISI, and (2) to design receivers capable of compensating for the ISI. The first group includes the simplest strategy, in which the transmitted pulses of the same frequency are separated in time far enough to ensure that all channel reverberation will die out before each subsequent pulse is to be received,[1] and the more complex systems which use spread-spectrum signals to reject multipath.[2] Both of these techniques sacrifice data throughput to eliminate the ISI. The more sophisticated systems of the second group allow for the ISI in the received data sequence, thus supporting high-speed communications through efficient use of the available bandwidth. Several types of channels, namely long-range deep and shallow water, and medium-range shallow water channels, have been shown to allow effective use of adaptive equalization methods for combating the ISI.[3]

A different approach to eliminating multipath propagation is the use of narrow beams, either at the transmitter or receiver end, which ensure that only a single deterministic propagation path contributes to the received signal. At the transmitter end, parametric sources which rely on the nonlinearity of transmission medium in front of a transducer, are used to excite only a single mode of propagation.[4,5] However, such sources are still considered impractical since in addition to pointing errors, their major limitation lies in high power requirements.[6] As an alternative to equalization, beamforming at the receiver end has been used to isolate the signal from a single propagation path based on its angular separation from undesired multipath.[5,7]

In addition to temporal variability, spatial variability of the ocean multipath represents a major problem for the single-channel receiver performance and motivates the use of multiple, spatially distributed sensors. Practical justification for investigating multichannel signal processing techniques lies in the relative simplicity of building large receiver arrays for applications such as UWA telemetry. Spatial diversity offers robustness to fading, provided that the beamforming and equalization techniques are properly combined, so as to exploit, rather than suppress the multipath propagation.

The use of spatial diversity combining for UWA communications was originally investigated for the case of nondispersive channels.[8] For frequency selective UWA channels, the design of the receivers which jointly perform spatial diversity combining and equalization, and their experimental performance results, were presented in Ref. 9. Recent references to multichannel equalization with applications to UWA

[a]Present address: Woods Hole Oceanographic Institution, Woods Hole, MA 02543.

 0001-4966/95/98(2)/961/12/$6.00

communications also include Ref. 10 which demonstrates the advantages of spatial diversity combining using a time-invariant simulation model for medium-range shallow water channels.

Although techniques for joint beamforming and equalization have been proposed for other communication channels,[11] their potential has not yet been fully recognized in application to UWA communications. The use of a beamformer and a single-channel equalizer as complementary devices was suggested in Ref. 12. It was found that while beamforming is effective for small range-to-depth ratios, an increase in range precludes angular multipath separation, necessitating the use of an equalizer. Similar conclusions are made in a recent overview of UWA communication systems[5] suggesting that the receiving strategy be moved from beamforming to equalization to diversity combining as the range increases relative to depth.

Multichannel, or spatial diversity equalization, analyzed in Ref. 9 represents a more general approach to spatial and temporal signal processing, effective for all range-to-depth ratios. This multichannel equalizer demonstrated superior performance over the single-channel case in configurations with only few channels. However, although it achieves near-optimal performance, its computational complexity significantly increases with the number of array sensors. This becomes a major limitation at high signaling rates when each of say, 20 input channels needs a 100-tap equalizer. Besides the increase in computational time, very large adaptive filters, which must operate with computationally efficient algorithms, imply increased sensitivity to numerical errors. Unfortunately, some of the fast RLS algorithms[13] preserve numerical stability only at the expense of sacrificing the tracking speed. As an alternative, a class of LMS algorithms with improved tracking properties has been proposed[14] for application in UWA equalization; however, its performance in the dynamic, nonstationary UWA environment still lacks the fast convergence properties of the RLS algorithms. Another disadvantage of large multichannel equalizers, and perhaps the critical one, lies in their increased noise enhancement, which significantly limits the gain obtained by increasing the number of channels.

These issues motivate the search for a different multichannel processing strategy in which the size of the adaptive filter will be reduced, but multipath diversity gain preserved. To this end, we start out in Sec. I by investigating the relationship between optimal diversity combining and beamforming. While beamforming is associated with large arrays, whose geometry permits them to reject interference by steering nulls in some directions, diversity combining can be performed with as few as two sensors, which only need to be separated far enough from each other to ensure independence of the received signals. Diversity combining alone does not account for channel equalization, and thus has to be used in conjunction with it. On the other hand, due to the large amount of multipath present in the UWA channels, an array could be used to repeatedly steer nulls in the directions of all but one signal reflection, and subsequently combine the ISI-free signals. In other words, a conventional beamformer, as termed in the array processing literature, would be used to cancel the unwanted signal interference,[7,15] while a diversity combiner, as found in communications literature, would try to make use of repetitive signal arrivals.[16,17] While there is a fundamental difference between the two techniques, both are used to mitigate ISI and fading caused by multipath propagation. We explore this fact to arrive at the optimal beamforming/combining strategy.

The analysis of optimal combining gives rise to two classes of adaptive implementations depending on whether knowledge of the spatial signal distribution is used by the receiver. The first class does not rely on such knowledge and corresponds to pure diversity combining.[9] The receivers of the second class exploit the fact that there exists a certain relationship between the array signals, and correspond to optimal beamforming. To compare the two approaches considered, a condition is derived in Sec. II for equivalence between a fully adaptive multichannel equalizer of the first class, and a less complex receiver which has perfect knowledge of the angles of multiple signal arrivals and uses it in a fixed beamformer. Performance of several beamforming strategies is studied on a simulation example, revealing that the interpretation of an optimal receiver as a beamformer and subsequent combiner leads to a receiver structure which significantly reduces the complexity of a pure diversity combiner, while achieving the same performance.

These ideas, derived from a narrow-band case, are extended in Sec. III to a broadband underwater acoustic communication scenario. In this case, the reduced-complexity receiver configuration is structurally suboptimal; nevertheless, it allows simultaneous optimization of the "beamformer" and the multichannel equalizer. Such an approach provides the desired reduction in complexity, and hence, improved algorithm stability and reduction in noise enhancement. An essential part of a practical receiver is a multichannel carrier phase estimator which provides necessary reference for coherent combining of multichannel signals. The key feature of the proposed algorithm is joint optimization of the combiner, or spatial processor, the multichannel decision-feedback equalizer (DFE) and the accompanying digital phase-locked loops (PLL), based on minimization of the mean-squared error (MSE) in the data detection process. The algorithm derivation is presented and the issues concerning its implementation are discussed.

Experimental results demonstrate excellent receiver performance on a long-range (50 nautical miles) shallow-water (about 50-m deep) channel off the New England Continental Shelf. We study cases of digital data transmitted at rates up to 2000 bits per second using 4- and 8-level phase shift keying (PSK), and received over a 20-element vertical array. The results lead us to conclude that the proposed class of reduced-complexity, but fully adaptive receivers for simultaneous beamforming and multichannel equalization is especially well-suited for real-time implementation in UWA modems.

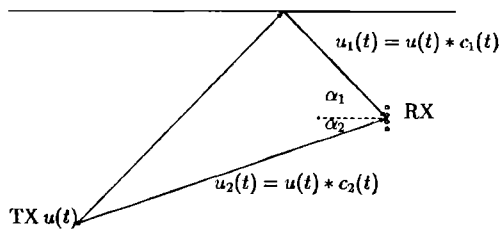

FIG. 1. Propagation model ($P=2$, $K=4$).

I. ADAPTIVE MULTICHANNEL PROCESSING: THE BEAMFORMING AND THE DIVERSITY COMBINING APPROACH

A. Propagation model

An acoustic channel can be modeled as consisting of a number of deterministic propagation paths, each described by an impulse response which takes into account any possible dispersion on the given deterministic path. We accordingly consider a channel in which the transmitted signal $u(t)$ propagates over a number of paths, P, each of which is characterized by its complex baseband impulse response $c_p(t)$. The multipath signal is received over K equally spaced sensors, as sketched in Fig. 1. To illustrate the model, we consider the simple narrow-band case, with ideal plane-wave propagation. In this case, the signal propagating via the pth path, $u_p(t) = u(t)*c_p(t)$, is observed at the kth sensor as $u_p(t)e^{-jk\varphi_p}$, where φ_p is the angle associated with the pth propagation path. The vector of the received signals is given as

$$\mathbf{v}(t)=\begin{bmatrix} v_0(t) \\ \vdots \\ v_{K-1}(t) \end{bmatrix}=\begin{bmatrix} 1 & \cdots & 1 \\ e^{-j\varphi_1} & \cdots & e^{-j\varphi_P} \\ \vdots & & \vdots \\ e^{-j(K-1)\varphi_1} & \cdots & e^{-j(K-1)\varphi_P} \end{bmatrix} \times \begin{bmatrix} u_1(t) \\ \vdots \\ u_P(t) \end{bmatrix} + \begin{bmatrix} n_0(t) \\ \vdots \\ n_{K-1}(t) \end{bmatrix}$$

$$=\mathbf{\Phi u}(t)+\mathbf{n}(t). \tag{1}$$

The noise components $n_k(t)$ are assumed to be independent of the signal. The signal $\mathbf{u}(t)$ depends on the underlying transmitted sequence of data symbols $\{d(n)\}$ as

$$\mathbf{u}(t)=\sum_n d(n)\mathbf{g}(t-nT), \tag{2}$$

where $\mathbf{g}(t)$ is the vector of overall path responses $g_p(t) = c_p(t)*g(t)$, which include all the transmitter and receiver filtering $g(t)$. With this notation, the received signal (1) is written as

$$\mathbf{v}(t)=\sum_n d(n)\mathbf{f}(t-nT)+\mathbf{n}(t), \tag{3}$$

where

$$\mathbf{f}(t)=\mathbf{\Phi g}(t) \tag{4}$$

is the vector of overall channel responses.

B. The role of beamforming in the optimal combiner

Assuming that the noise vector $\mathbf{n}(t)$ is zero-mean, temporally white, Gaussian, with a known covariance $\mathbf{R}_n$, the optimal, maximum likelihood (ML) receiver consists of a combiner and a postprocessor for detecting the transmitted data sequence.[9] The optimal combiner incorporates a bank of K matched filters with impulse responses $f_k^*(-t)$, whose outputs are summed and sampled at the signaling rate. The combiner output, produced at discrete intervals of time nT, is given by (prime denotes conjugate transpose)

$$y(n)=\int_{T_{\text{obs}}} \mathbf{f}'(t-nT)\mathbf{R}_n^{-1}\mathbf{v}(t)dt \tag{5}$$

and it constitutes the decision variable for determining the transmitted sequence $\{d(n)\}$. Regardless of the detection process, which can be realized as maximum-likelihood sequence estimation or some form of sequential detection based on equalization, the combining process is described by Eq. (5). Since we are primarily concerned with the combining problem, we shall stay with linear equalization methods, as the simplest to analyze, for the rest of our present discussion. A practical receiver, based on decision-feedback equalization which is especially suitable for UWA signal processing, will be described in Sec. III.

So far, we have made no assumptions about the spatial distribution of signals across the array. Should there exist a relationship between signals observed at different sensors, the optimal combiner has a special interpretation. For the narrow-band case and plane-wave propagation, for which the spatial signal distribution is given by (4), the output of the optimal combiner can be represented as

$$y(n)=\int_{T_{\text{obs}}} \mathbf{g}'(t-nT)\mathbf{\Phi}'\mathbf{R}_n^{-1}\mathbf{v}(t)dt. \tag{6}$$

This expression implies a different combiner structure in which the parts corresponding to "beamforming," and those corresponding to matched filtering and coherent combining are clearly separated. The beamforming part is identified as depending only on the angles of signal arrivals, and is represented by a $K\times P$ beamforming matrix $\mathbf{\Phi}$. The P signals at its output are associated with the P propagation paths, and the P filters are matched to the individual path responses $g_p(t)$. The gain obtained in the optimal combiner in the case of uncorrelated multipath is proportional both to the number of sensors and to the number of propagation paths.

C. Two classes of adaptive combiners

Although theoretically identical, the two combiner structures discussed give rise to different adaptive implementations depending on whether knowledge of the spatial signal distribution is available at the receiver. If the receiver has no information about the angles of signal arrivals, a pure K-channel diversity combiner of Fig. 2 can be implemented. Alternatively, a beamformer followed by a P-channel equalizer can be chosen as shown in Fig. 3 if the spatial signal distribution $\mathbf{\Phi}$ is known.

In practice, the matched filters, symbol-synchronous sampling and the linear part of the equalizer will be realized

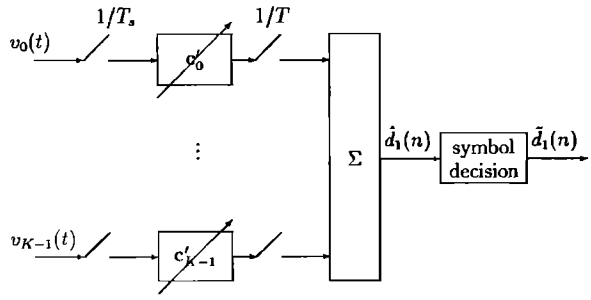

FIG. 2. Adaptive receiver with K-channel equalizer.

together in a bank of fractionally spaced adaptive filters of finite length. Accordingly, we consider optimizing the finite length receivers based on minimization of the MSE between the true and the estimated data symbol,

$$\mathrm{MSE}=E\{|d(n)-\hat{d}(n)|^2\}. \tag{7}$$

Referring to Figs. 2 and 3, the estimated data symbols of the two receivers are given by

$$\hat{d}_1(n)=\mathbf{c}'\mathbf{v}[n] \tag{8}$$

$$\hat{d}_2(n)=\mathbf{a}'\mathbf{w}[n]. \tag{9}$$

The equivalent input signal vector $\mathbf{v}[n]$ for the full K-channel equalizer consists of the vectors $\mathbf{v}_k[n]$ of the T_s-spaced received signal samples currently stored in the kth equalizer, and the equivalent input signal vector $\mathbf{w}[n]$ for the P-channel equalizer is composed of the vectors

$$\mathbf{w}_p[n]=[\mathbf{v}_0[n]\cdots\mathbf{v}_{K-1}[n]]\mathbf{b}_p^*=\mathbf{V}[n]\mathbf{b}_p^*, \tag{10}$$

where $\mathbf{b}_p$ is the pth column of $\mathbf{B}$. Guided by the structure of the optimal receiver, in the case of spatially white input noise, the beamforming transformation will be chosen as $\mathbf{B}=\mathbf{\Phi}$.

The MMSE solutions for the overall equalizer tap-weight vectors are given by

$$\mathbf{c}=\mathbf{R}_{vv}^{-1}\mathbf{R}_{vd}, \tag{11}$$

$$\mathbf{a}=\mathbf{R}_{ww}^{-1}\mathbf{R}_{wd}, \tag{12}$$

where the notation $\mathbf{R}_{xy}=E\{\mathbf{x}[n]\mathbf{y}'[n]\}$ is used to denote the cross correlations. Hence, any form of adaptive, decision-directed algorithm can be applied to the signals $\mathbf{v}[n]$ and $\mathbf{w}[n]$ to obtain the multichannel equalizer tap-weights $\mathbf{c}$ and $\mathbf{a}$, respectively.

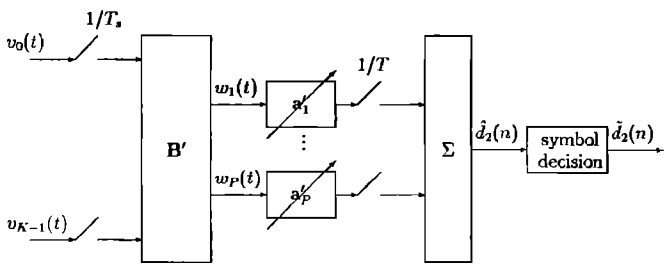

FIG. 3. Adaptive receiver with beamformer and P-channel equalizer.

1. Joint adaptive equalization and angle of arrival tracking

So far we have assumed that the receiver has knowledge of the angles of arrival, or their estimates, which it uses in a fixed beamformer. However, because of the relative motion between the receiver and the transmitter, the true angles of arrival will change with time. A tracking algorithm for the estimates $\{\hat{\varphi}_p\}$ can be obtained by exploiting the special structure of the transformation $\mathbf{B}=\hat{\mathbf{\Phi}}$ which corresponds to the optimal combiner's beamforming part.

To find the MMSE estimates of the angles $\{\hat{\varphi}_p\}$ which are jointly optimal with the equalizer vectors $\{\mathbf{a}_p\}$, it is convenient to use the shorthand notation

$$P_{p,k}=\mathbf{a}_p'\mathbf{v}_k[n], \quad P_p(\varphi)=\sum_{k=0}^{K-1}P_{p,k}e^{jk\varphi}. \tag{13}$$

The error $e(n)=d(n)-\hat{d}(n)$ can now be expressed in terms of $\hat{\varphi}_p$ as

$$e(n)=d(n)-\sum_{i\neq p}P_i(\hat{\varphi}_i)-P_p(\hat{\varphi}_p)=Q_p-P_p(\hat{\varphi}_p), \tag{14}$$

where Q_p is independent of $\hat{\varphi}_p$. Differentiating the MSE with respect to $\hat{\varphi}_p$, we obtain

$$\frac{\partial\mathrm{MSE}}{\partial\hat{\varphi}_p}=-2\ \mathrm{Re}\{E\{\dot{P}_p(\hat{\varphi}_p)e^*(n)\}\},$$

$$\dot{P}_p(\varphi)=\frac{\partial P_p(\varphi)}{\partial\varphi}=j\sum_{k=1}^{K-1}kP_{p,k}e^{jk\varphi}=jF_p(\varphi). \tag{15}$$

With this notation, the MMSE solution $\hat{\varphi}_p$ has to satisfy

$$\frac{\partial\mathrm{MSE}}{\partial\hat{\varphi}_p}=2\ \mathrm{Im}\{E\{F_p(\hat{\varphi}_p)[Q_p-P_p(\hat{\varphi}_p)]^*\}\}=0. \tag{16}$$

An important difference between the two classes of adaptive receivers now becomes evident. Because of the constrained structure of the matrix $\hat{\mathbf{\Phi}}$, the expression (16) has no closed form solution. At the same time, the tap-weights $\mathbf{c}$ of the fully adaptive K-channel equalizer have the closed-form MMSE solution (11).

To obtain a recursive solution for the angles $\{\hat{\varphi}_p\}$, we define the angular error at iteration n as

$$\psi_p(n)=\mathrm{Im}\{F_p(\hat{\varphi}_p(n))e^*(n)\}, \quad p=1,\ldots,P. \tag{17}$$

The current estimate $\hat{\varphi}_p(n)$ can then be updated as

$$\hat{\varphi}_p(n+1)=\hat{\varphi}_p(n)-K_1\psi_p(n)-K_2\sum_{m=0}^{n}\psi_p(m),$$

$$p=1,\ldots,P \tag{18}$$

with appropriately chosen angle-tracking constants K_1, K_2, and initial values of the estimates. The outlined solution is analogous to a second-order digital PLL. Note, however, that (18) represents only the angle-locked loop, and that for practical applications, an additional carrier phase tracking loop might have to be associated with each of the propagation paths to compensate for their carrier frequency distortions.

II. COMPARISON OF COMBINERS

If the number of sensors is larger than the number of propagation paths, the class of receivers which rely on the spatial signal distribution has a lower computational complexity. For applications such as high-rate telemetry over severely dispersive channels, any reduction in comp'exity becomes extremely important. On the other hand, a fully adaptive K-channel equalizer has the main advantage in not requiring any *a priori* knowledge of the spatial distribution of signals, such as the number of multiple arrivals. It is therefore insensitive to any model mismatch, in the sense that it implicitly estimates the model parameters during the process of adaptation. Hence, a question arises as to whether there are beamforming strategies which could perform equally well but are not constrained on the explicit knowledge of propagation conditions.

A. Condition for equivalence between the two classes of combiners

Now we wish to compare the performance of a fully adaptive K-channel equalizer to that of a reduced-complexity structure which employs an arbitrary $K\times P$ beamforming matrix $\mathbf{B}$ and an adaptive P-channel equalizer. We assume a stationary environment, described by fixed angles of signal arrivals.

The input signal vector $\mathbf{w}[n]$ for the reduced-complexity receiver of Fig. 3 is expressed in terms of the input signal $\mathbf{v}[n]$ as

$$\mathbf{w}[n]=\mathbf{B}_N'\mathbf{v}[n],\quad \mathbf{B}_N'=\begin{bmatrix} b_{11}^*\mathbf{I}_N & \cdots & b_{K1}^*\mathbf{I}_N \\ \vdots & & \vdots \\ b_{1P}^*\mathbf{I}_N & \cdots & b_{KP}^*\mathbf{I}_N \end{bmatrix}. \tag{19}$$

The elements $\{b_{pk}\}$ constitute the beamforming matrix $\mathbf{B}$, and $\mathbf{I}_N$ is the identity matrix of size N equal to the number of equalizer tap weights in each branch. The matrix $\mathbf{B}_N$ is thus obtained by "expanding" the matrix $\mathbf{B}_1=\mathbf{B}$. Using the expression (19), the cross correlations which determine the optimal receivers (11) and (12) are related by

$$\mathbf{R}_{wd}=\mathbf{B}_N'\mathbf{R}_{vd},\quad \mathbf{R}_{ww}=\mathbf{B}_N'\mathbf{R}_{vv}\mathbf{B}_N. \tag{20}$$

From (3), the input signal vector can be expressed as

$$\mathbf{v}[n]=\mathbf{\Phi}_N\sum_m d(m)\mathbf{g}[n-m]+\mathbf{n}[n], \tag{21}$$

where $\mathbf{\Phi}_N$ is the Nth expansion of $\mathbf{\Phi}$, and $\mathbf{g}[m]$ consists of P vectors of T_s-sampled path responses, shifted by m symbol intervals with respect to the center vector $\mathbf{g}[0]=\mathbf{g}$. Using this representation, the signal covariance is obtained as

$$\mathbf{R}_{vv}=\mathbf{\Phi}_N[\mathbf{g}\mathbf{g}'+\mathbf{G}]\mathbf{\Phi}_N'+\mathbf{R}_{nn}=\mathbf{\Phi}_N\mathbf{g}\mathbf{g}'\mathbf{\Phi}_N'+\mathbf{N}, \tag{22}$$

where

$$\mathbf{G}=\sum_{m\neq 0}\mathbf{g}[m]\mathbf{g}'[m] \tag{23}$$

defines the noise term associated with ISI.

The steady-state MSE achieved by the K-channel equalizer is now given by

$$\mathrm{MMSE}_K=1-\mathbf{R}_{vd}'\mathbf{R}_{vv}^{-1}\mathbf{R}_{vd}=1/[1+\mathbf{g}'\mathbf{\Phi}_N'\mathbf{N}^{-1}\mathbf{\Phi}_N\mathbf{g}]. \tag{24}$$

Similarly, using the expressions (20), the MMSE achieved by the smaller P-channel equalizer is

$$\mathrm{MMSE}_P=1-\mathbf{R}_{wd}'\mathbf{R}_{ww}^{-1}\mathbf{R}_{wd}$$
$$=1/[1+\mathbf{g}'\mathbf{\Phi}_N'\mathbf{B}_N(\mathbf{B}_N'\mathbf{N}\mathbf{B}_N)^{-1}\mathbf{B}_N'\mathbf{\Phi}_N\mathbf{g}]. \tag{25}$$

We shall say that the two structures are equivalent if they achieve the same MMSEs. In order for the equivalence to hold for arbitrary path responses $\mathbf{g}$, the following relation must hold

$$\mathbf{\Phi}_N'\mathbf{B}_N(\mathbf{B}_N'\mathbf{N}\mathbf{B}_N)^{-1}\mathbf{B}_N'\mathbf{\Phi}_N=\mathbf{\Phi}_N'\mathbf{N}^{-1}\mathbf{\Phi}_N. \tag{26}$$

Since all the required inverses are those of covariance matrices, we can assume their existence, and substitute for the overall noise covariance $\mathbf{N}$ as defined by Eq. (22), to obtain the equivalent relationship

$$\mathbf{\Phi}_N'\mathbf{B}_N(\mathbf{B}_N'\mathbf{R}_{nn}\mathbf{B}_N)^{-1}\mathbf{B}_N'\mathbf{\Phi}_N=\mathbf{\Phi}_N'\mathbf{R}_{nn}^{-1}\mathbf{\Phi}_N. \tag{27}$$

To further simplify the obtained expression, we use the fact that the Nth expansions of any matrices $\mathbf{X}$ and $\mathbf{Y}$ satisfy $\mathbf{X}_N\mathbf{Y}_N=(\mathbf{XY})_N$ and, hence, for a square matrix, $\mathbf{X}_N^{-1}=(\mathbf{X}^{-1})_N$. In the case of white input noise, the condition (27) finally reduces to

$$\mathbf{\Phi}'\mathbf{B}(\mathbf{B}'\mathbf{B})^{-1}\mathbf{B}'\mathbf{\Phi}=\mathbf{\Phi}'\mathbf{\Phi}. \tag{28}$$

Whenever the chosen beamformer $\mathbf{B}$ satisfies this simple condition, the performance of the reduced-complexity receiver will equal that of the full K-channel equalizer. This is an interesting conclusion since it says that any kind of beamforming, which satisfies the condition (28), can be used to reduce the computational complexity of the full multichannel equalizer. In other words, it is not necessary to use $\mathbf{B}=\mathbf{\Phi}$ of the optimal combiner, since as long as (28) is satisfied, the P-channel equalizer will be able to achieve the overall MMSE solution. By inspection, we see that the optimal combiner's beamformer $\mathbf{B}=\mathbf{\Phi}$ satisfies the equivalence condition (28). This is also true for the conventional beamformer[15] $\mathbf{B}=\mathbf{\Phi}(\mathbf{\Phi}'\mathbf{\Phi})^{-1}$, which produces at its output an estimate of the spatially separated signals $\mathbf{u}(t)$. In fact, whenever $\mathbf{B}$ can be expressed as a product of the angle matrix $\mathbf{\Phi}$ and an arbitrary invertible matrix, it will satisfy the equivalence condition. The necessary condition for the equivalence (28) to hold is that the size of the matrix $\mathbf{B}$, i.e., the reduced number of channels to be equalized, not be smaller than the number of propagation paths.

B. Reduced-complexity unconstrained combining

While the two approaches considered in Sec. I represent two extremes, the above analysis encourages us to combine them, in order to reduce the computational complexity of the fully adaptive multichannel equalizer, but make no explicit assumptions about the underlying spatial signal distribution. This can be accomplished by using a $K\times P$ adaptive beamformer of unconstrained structure, together with a P-channel equalizer. In fact, P here does not have to have the same physical meaning as in the optimal combiner structure. Joint

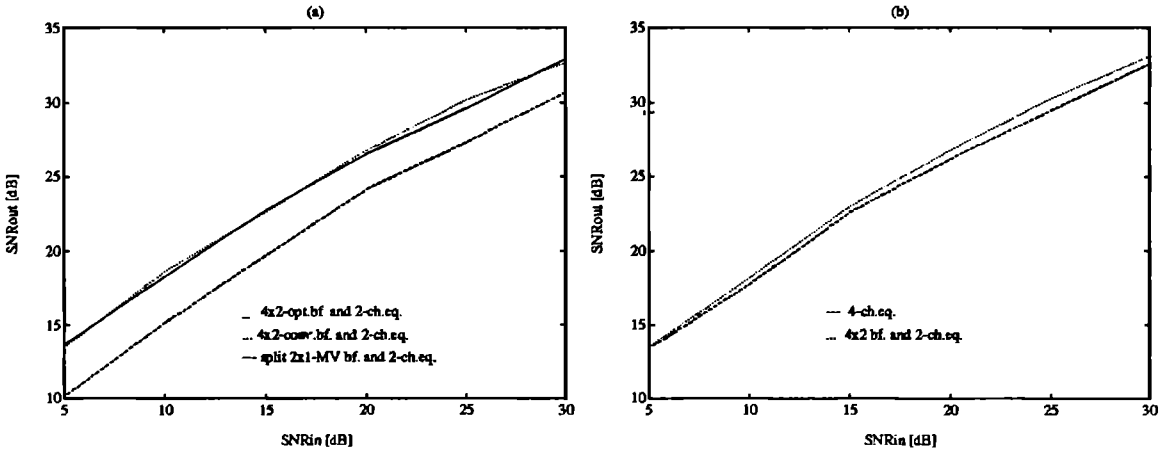

FIG. 4. Performance comparison of (a) fixed beamformers and (b) fully adaptive receivers.

optimization of the beamformer and the equalizer elements will ensure the MMSE performance of the given receiver structure. A special case with $P=1$ was analyzed in Ref. 11 which gives an interesting analysis of the shared tasks of beamforming and equalization.

The optimal MMSE value of the overall beamforming vector $\mathbf{b}' = [\mathbf{b}_1' \cdots \mathbf{b}_P']$ is given by

$$\mathbf{b}=\mathbf{R}_{uu}^{-1}\mathbf{R}_{ud}, \tag{29}$$

where $\mathbf{u}[n]$ is comprised of the equivalent input signals to the beamformer,

$$\mathbf{u}_p[n]=\mathbf{V}^T[n]\mathbf{a}_p^*, \quad p=1,\ldots,P. \tag{30}$$

The beamformer coefficients (29) and the equalizer coefficients $\mathbf{a}$ from (12) will be used together to obtain the algorithm for joint adaptation of the beamformer and the equalizer, as described in more detail in the following section.

With each of the equalizers having length N, a total of $K\times P+P\times N$ taps have to be computed per iteration, as opposed to the $K\times N$ taps of the full diversity combiner.

Although this receiver structure resembles a subarray beamformer,[18] both the matrix beamformer and the reduced-complexity multichannel equalizer remain adaptive. As long as there exists an underlying spatial signal distribution which permits the decomposition of the optimal combiner into the beamformer and the reduced-complexity equalizer, no performance degradation need result from the reduction in complexity.

C. Simulation example

The purpose of this simulation is to illustrate the impact of the choice of a combining strategy on the receiver performance and its complexity. Consider a simple example with $P=2$ propagation paths, $K=4$ array sensors, and spatially white noise. Assuming that the angles φ_1 and φ_2 are known, we compare several possible beamforming strategies. A matrix beamformer is chosen either in an optimal fashion, $\mathbf{B}=\mathbf{\Phi}$, or as a conventional beamformer, $\mathbf{B}=\mathbf{\Phi}(\mathbf{\Phi}'\mathbf{\Phi})^{-1}$. An alternative approach to resolving the two signal arrivals is to group the elements of the array into two groups, dedicating each group to beamforming toward one of the arrivals. Note that this approach is somewhat similar to space-beam processing, another strategy used in array processing to reduce the computational complexity of fully adaptive arrays.[15] A minimum of $K=4$ elements is needed for such split beamforming. Each of the two beamformers can use any of the classical criteria for interference suppression. Minimum variance (MV), MMSE, or ML criteria differ only by a scalar factor,[15] and are equivalent from a data-detection point of view. Regardless of the optimization method for the two-element beamforming vectors $\mathbf{b}_{11}$ and $\mathbf{b}_{22}$, the overall beamforming matrix

$$\mathbf{B}=\begin{bmatrix}\mathbf{b}_{11} & \mathbf{0}\\ \mathbf{0} & \mathbf{b}_{22}\end{bmatrix} \tag{31}$$

will not satisfy the condition (28). Hence, split beamforming cannot achieve the performance of nonrestricted, full-matrix beamforming.

The performance of these three fixed beamformers operating with a 2-channel adaptive equalizer is illustrated through the simulation results shown in Fig. 4(a). The following parameters were used:

modulation: QPSK
transmitter and receiver pulse: raised cosine (roll-off 0.5, total duration 4 T)
differential path delay: 2.5 T
path power ratio: 1
array element spacing: $d=\lambda/2$
angles of arrival: $\alpha_1=30°$; $\alpha_2=-20°$
equalizer: 13 taps, $T/2$-spaced
adaptive algorithm: RLS.

The receiver performance is quantified through the steady-state output SNR, $\mathrm{SNR}_{\mathrm{out}}=10\log(1/\mathrm{MMSE})$. Each simulation run corresponded to the transmission of a 1000-symbol data block, for which the MSE is obtained as a 500-symbol time-average of the instantaneous squared error observed in the steady state, i.e., at the end of the data block after the convergence has been established. The so-obtained values were ensemble-averaged over 100 simulation runs, to obtain the final value of the steady-state MSE.

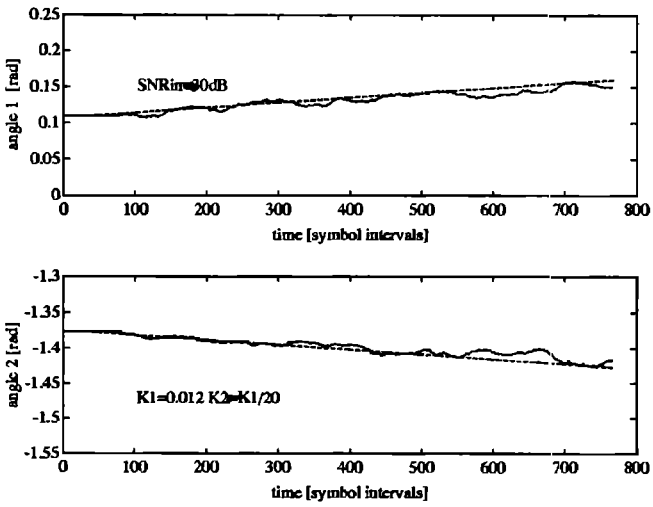

FIG. 5. Tracking performance of the angle-locked loop.

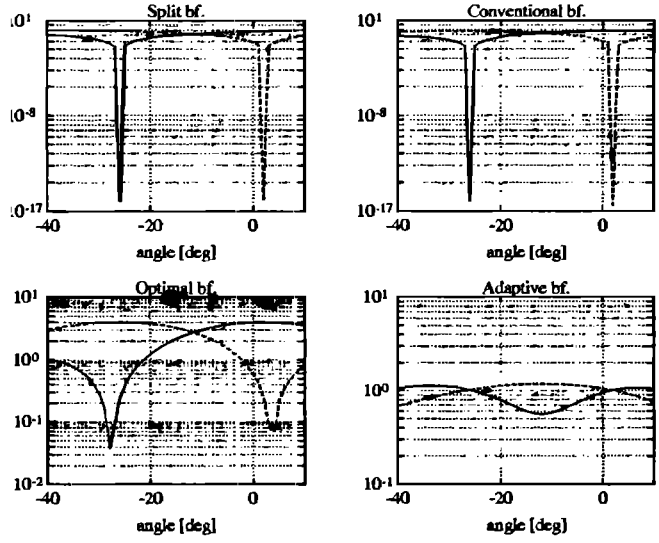

FIG. 6. Beampatterns of various combiners.

Figure 4(a) represents the steady-state output SNR as a function of the input SNR. The two upper curves correspond to the full-matrix beamformers, and the lower curve corresponds to the split beamformer. Each of the two split beamformers is optimized according to the MV criterion. The performance in the latter case is about 3 dB worse throughout the range of the SNRs presented, while the adaptive equalizers of both full-matrix beamformers achieve the same performance. An advantage of the optimal over the conventional beamformer is that it cannot become numerically ill-conditioned.

When the angles of arrival are not known, a fully adaptive receiver is needed. It can either be realized as a 4-channel equalizer, or as a jointly adaptive 4×2 beamformer and a 2-channel equalizer. None of these structures requires explicit knowledge of the angles of signal arrivals. The performance of the two receivers is shown in Fig. 4(b). Not only does the reduced-complexity receiver achieve the same performance as the unconstrained diversity combiner, but their performance is equal to that of the fixed matrix beamformers of Fig. 4(a). This demonstrates the possibility of achieving a reduction in complexity by carefully designing an adaptive receiver to match the propagation conditions. For K several times greater than P, and a large number of equalizer tap weights, a significant reduction in complexity will be achieved. A slight degradation observed in performance of the full K-channel equalizer is explained by its higher noise enhancement.

In practice, the angles of signal arrivals will be time varying. While both of the fully adaptive receivers are capable of tracking these variations, additional estimation of the angles of arrival will have to be incorporated into the receiver which relies on the $\mathbf{B}=\hat{\mathbf{\Phi}}$ type of beamforming. Figure 5 illustrates the performance of the angle-tracking algorithm described in Sec. I. The time variation of the angles of arrival $\alpha_{1,2}$ is modeled as being the result of the vertical motion of the receiver at a constant speed of 5 m/s. The fastest changes in the angles of arrival will occur at lower ranges and, relative to the update interval of one symbol duration, at lower signaling rates. For a shallow water channel, with the transmitter depth of 30 m, the receiver depth of 10 m, and a range of only 100 m, simple geometry shows that the direct-path and the surface-reflection angles of arrival will change at the rate of about $\pm2.5°$/s. The angle-tracking results shown in Fig. 5 correspond to signaling over such a channel, at 2000 symbols per second. Note that in practice much higher rates can be achieved over this channel. The dashed curves represent the true values of the angles $\varphi_{1,2}=\pi \sin \alpha_{1,2}$, and the solid curves represent their estimates, obtained jointly with those of the equalizer coefficients. The tracking performance of the algorithm is very good, resulting in the same steady-state MSE as that of the unconstrained beamformer. However, as opposed to the jointly adaptive unconstrained beamformer and equalizer, this type of algorithm is very sensitive to the initial values of the angle estimates, as well as to the choice of the angle-tracking constants. In return, it requires only P angle estimates in contrast to estimating the $K\times P$ elements of an unconstrained beamformer.

Describing the performance of the beamformers by their beampatterns is not as meaningful from a data-detection point of view as it is from the viewpoint of interference cancellation because the beamformer and the multichannel equalizer are optimized jointly to achieve the best MSE performance. Hence, the task of ISI-suppression is shared between them. To illustrate this, Fig. 6 shows the beampatterns of several beamformers used. The angles of arrival of 2° and −26° correspond to the above-mentioned shallow water scenario. Only the conventional and the split beamformer have any deep nulls placed interchangeably in the directions of the two signal arrivals. Rather than by nulls, the optimal beamformer is characterized by the points of maxima, which it places in the directions of the two signal arrivals. Finally, the beampattern of the unconstrained adaptive beamformer in steady-state indicates neither distinct minima nor distinct maxima. This is easily understood from the fact that the solution for the beamforming matrix $\mathbf{B}$ is not unique. Any so-

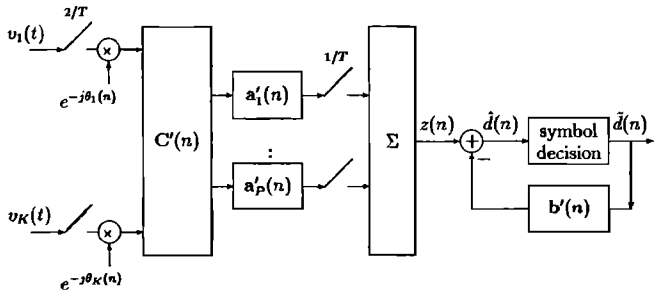

FIG. 7. Reduced-complexity multichannel DFE.

lution, which together with the underlying solution for the equalizer coefficients results in the minimal MSE, is equally good from the data-detection point of view.

III. REDUCED-COMPLEXITY COHERENT COMBINING AND MULTICHANNEL DECISION-FEEDBACK EQUALIZATION

Because of the fundamental bandwidth limitations of the UWA channels, high-speed communications over these channels are inherently broadband. Hence, the full-complexity multichannel processor is the optimal choice for this case. Nevertheless, there are many practical advantages of using the "beamforming"/equalization approach, even if it represents a structurally suboptimal solution. Joint, unconstrained optimization of the spatial and temporal processor parts will ensure best performance of the chosen receiver structure, providing at the same time the needed reduction in complexity.

A reduced-complexity combiner can be used in conjunction with any type of equalization method (linear, DFE or ML sequence estimation). We focus on a multichannel DFE, as it has proven to be an adequate choice for UWA channels characterized by extremely long impulse responses.[3]

A. Receiver structure and algorithm

The complete structure of a practical receiver is shown in Fig. 7. The complex baseband input signals $v_k(t)$, $k=1,\ldots,K$, are assumed to be bandlimited to the signaling rate $1/T$, and frame synchronized prior to sampling at twice the signaling rate ($T_s=T/2$). The front part of the practical receiver is equipped by a multichannel digital PLL which enables coherent combining. In cases when sufficient coherency between phases can be expected, phase correction can be performed at a point after combining using only P distinct phase estimates, or only a single phase estimate for all the channels can be used. These modifications are easy to carry out, and we concentrate on the case when all K phase estimates are computed. The $K\times P$ combiner performs spatial signal processing only, while temporal processing and final combining are performed in a bank of P feedforward equalizers. Receiver parameters are updated once per symbol interval and the output of the linear part of the receiver is accordingly delivered to the feedback section. The receiver parameters to be optimized are defined below:

$\{\theta_k\}_{k=1}^{K}$: carrier phase estimates,

$\{\mathbf{c}_p\}_{p=1}^{P}$: combiner ("beamformer") vectors with K elements $[c_{k,p}]_{k=1,\ldots,K}$,

$\{\mathbf{a}_p\}_{p=1}^{P}$: feedforward equalizer vectors with N elements $[a_{i,p}]_{i=-N_1,\ldots,N_2}$,

$\mathbf{b}$: feedback filter tap-weight vector with M elements.

Assuming initially that the channel is fixed over some interval of time, one arrives at the optimal values of the receiver parameters.[9] Tracking of the optimal solution is accomplished through a second-order gradient update for the multichannel PLL and a double application of the RLS algorithm for obtaining the combiner coefficients and the coefficients of a multichannel DFE. Since the receiver parameters are optimized jointly, the overall adaptation algorithm relies on the single error, $e(n)=d(n)-\hat{d}(n)$.

After compensating for the carrier phase distortions, the input signal samples at time nT are represented in the matrix form

$$\mathbf{V}[n]=[\mathbf{v}_1[n]e^{-j\theta_1}\cdots\mathbf{v}_K[n]e^{-j\theta_K}], \tag{32}$$

where

$$\mathbf{v}_k[n]=\begin{bmatrix} v_k(nT+N_1T/2) \\ \vdots \\ v_k(nT-N_2T/2) \end{bmatrix}. \tag{33}$$

The estimated data symbol, which is the input to the decision device, is given by

$$\hat{d}(n)=z(n)-\mathbf{b}'\tilde{\mathbf{d}}(n), \tag{34}$$

where $z(n)$ represents the output of the linear part of the receiver after coherent combining, and $\tilde{\mathbf{d}}(n)$ is the vector of M previously detected symbols stored in the feedback filter.

To obtain the carrier phase update equations it is useful to represent the variable $z(n)$ as

$$z(n)=\sum_{k=1}^{K} A_k(n)e^{-j\theta_k}, \quad A_k(n)=\sum_{p=1}^{P} c_{k,p}^{*}\mathbf{a}_p'\mathbf{v}_k[n]. \tag{35}$$

This representation leads to the definition of the equivalent PLL detector outputs as

$$\Phi_k(n)=\mathrm{Im}\{A_k(n)e^{-j\theta_k}e^{*}(n)\}, \quad k=1,\ldots,K. \tag{36}$$

Application of the stochastic gradient method yields the second-order carrier phase update equations

$$\theta_k(n+1)=\theta_k(n)+K_{f_1}\Phi_k(n)+K_{f_2}\sum_{m=0}^{n}\Phi_k(m), \tag{37}$$

where $K_{f_{1,2}}$ are the phase tracking constants. Similarly as in the full-complexity multichannel equalizer case, successful operation of the entire receiver strongly depends on the use of a second-order phase update in each of the K channels because of the severe phase fluctuations observed in many of the UWA channels.[9]

MMSE optimization of the combiner/equalizer parameters requires that their equivalent input data vectors be defined. To do so, the variable $z(n)$ is represented in two ways:

$$z(n)=[\mathbf{c}_1'\cdots\mathbf{c}_P']\begin{bmatrix}\mathbf{V}^T[n]\mathbf{a}_1^*\\ \vdots\\ \mathbf{V}^T[n]\mathbf{a}_P^*\end{bmatrix}=\mathbf{c}'\mathbf{u}[n], \tag{38}$$

or

$$z(n)=[\mathbf{a}_1'\cdots\mathbf{a}_P']\begin{bmatrix}\mathbf{V}[n]\mathbf{c}_1^*\\ \vdots\\ \mathbf{V}[n]\mathbf{c}_P^*\end{bmatrix}=\mathbf{a}'\mathbf{w}[n]. \tag{39}$$

The last expressions define the needed data vectors: $\mathbf{u}[n]$, the equivalent input to the combiner, and $\mathbf{w}[n]$, the equivalent input to the multichannel feedforward equalizer. An RLS type of algorithm is used to update the combiner vector $\mathbf{c}(n)$, as directed by the input data $\mathbf{u}[n]$ and the error $e(n)$. A second RLS update is used for the overall equalizer vector

$$\mathbf{f}(n)=\begin{bmatrix}\mathbf{a}(n)\\ -\mathbf{b}(n)\end{bmatrix}. \tag{40}$$

The input data for this update is a composite vector

$$\mathbf{x}[n]=\begin{bmatrix}\mathbf{w}[n]\\ \tilde{\mathbf{d}}(n)\end{bmatrix}, \tag{41}$$

while the error remains the same. Assuming correct decisions, the desired MMSE solutions are given by

$$\mathbf{c}=[E\{\mathbf{u}[n]\mathbf{u}'[n]\}]^{-1}E\{\mathbf{u}[n](d(n)+\mathbf{b}'\tilde{\mathbf{d}}(n))^*\} \tag{42}$$

and

$$\mathbf{f}=[E\{\mathbf{x}[n]\mathbf{x}'[n]\}]^{-1}E\{\mathbf{x}[n]d^*(n)\}. \tag{43}$$

Because there is no unique solution for the combiner/equalizer coefficients, i.e., there are infinitely many solutions which lead to the global minimum of the MSE, proper initialization must be used to set the starting point outside the region of a local minimum, e.g., not all the coefficients can be taken to be zero. Section II discussed possible solutions for the combiner which allow the equalizer coefficients to reach the jointly optimal solution in the case of a stationary environment with fixed and known angles of signal arrivals from multiple propagation paths. One of these solutions is to choose each of the beamforming vectors $\mathbf{c}_p$ equal to the steering vector corresponding to the pth propagation path. However, since it is unlikely that such detailed knowledge about propagation conditions will be available at the receiver, a more general initialization procedure is desired. Without showing its optimality, we have found the following initialization procedure to yield good results. At the start of adaptation, the combiner value is kept fixed at an initial value, while the equalizer coefficients are updated from an all-zero condition. When the equalizer has converged (in a time interval corresponding to about twice the number of its taps), the beamformer begins its update. The initial values of the beamformer vectors $\mathbf{c}_p$ can be chosen to have all zeros and a one at position p. In this way, the beamformer initially passes to the equalizer the P arbitrarily chosen channels, without processing them. Later, it gains access to all K channels, and begins their combining toward reducing the output MSE.

Since a separate update is used for the combiner and the equalizer, both the type of algorithm and the rate of its convergence can be chosen independently for the two updates. When very long channel responses are to be equalized, the multichannel DFE operates under a fast, numerically stable RLS.[13] On the other hand, the combiner's algorithm can be chosen even as standard RLS when KP is small enough to justify such choice. A choice of slightly different RLS forgetting factors, which allows faster convergence of the combiner, may help improve the convergence rate of the overall algorithm.

With currently available processing speeds, and relatively low candidate symbol rates for long-range UWA telemetry, computational complexity of fast RLS algorithms allows a moderate number of channels to be processed in real-time. (With 50 Mflops, and equalizer lengths on the order of several tens, which is representative of 500–1000 symbols per second transmissions used in the experiment described below, less than ten channels can theoretically be accommodated.) Although the increased number of channels allows shorter feedforward equalizers to be used, this does not alleviate the computational complexity problem. At shorter ranges, which support much higher data rates, the allowable number of channels reduces to only a few, making the use of reduced-complexity receivers, together with computationally efficient algorithms, imperative for processing a large number of channels.

Even when the computational complexity allows the use of optimal, full-complexity multichannel equalization, with increased number of taps to be updated, numerical stability imposes additional restrictions for use of the fastest RLS algorithms. To preserve stability, the forgetting factor of this algorithm has to be chosen[13] roughly as $\lambda>1-1/(2\times$ total number of taps). While for a small number of taps, allowable values of λ lie well within the region of practical interest (say, $\lambda\geq 0.98$), for large number of taps, λ becomes confined to relatively large values. (For 100 feedforward taps, 100 feedback taps, and say, 4 channels, it has to be $\lambda>0.999$.) These values may be too high to provide adequate tracking for many of the UWA channels. In such a case, reduced-complexity multichannel processing provides an alternative to using other types of RLS algorithms, such as lattice algorithms, which are inherently stable at the expense of increased complexity.

Finally, noise enhancement in large adaptive filters represents a serious problem for full-complexity multichannel equalization.[9] The reduced-complexity approach plays a vital role in this case, since it enables the multiple sensor signals to be combined prior to equalization, thus additionally exploiting the spatial variability of the ocean channel. Equalizing the so-obtained smaller number of signals has the important feature of keeping the noise enhancement at a minimum.

B. Experimental results

The reduced-complexity multichannel equalization method was tested for application in long-range UWA telemetry. The algorithm described in this section was used to process the data obtained during a May 1992 experiment conducted by the Woods Hole Oceanographic Institution at the New England Continental Shelf. In this experiment, a vertical receiver array of 20 sensors was deployed between

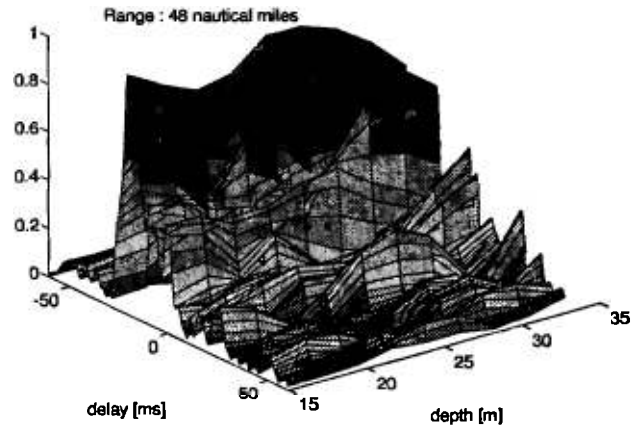

FIG. 8. Long-range shallow water channel responses at different depths.

15 and 35 m in about 50-m deep water, and transmissions were conducted at ranges of 15 to 65 nautical miles. With a transmitter power of 193 dB *re*:μPa, a 1-kHz carrier was used to transmit 4- and 8-PSK modulated signals at rates up to 1000 symbols per second (sps). A cosine roll-off filter with roll-off factor 0.5 was used to shape the signals at the transmitter.

As an example, we shall study the case of a 500 sps 8-PSK transmission over 48 nautical miles. Spatial variability of the long-range shallow water channel at 48 nautical miles is illustrated in Fig. 8. Shown in the figure are the instantaneous channel responses as a function of receiver depth. Clearly, there is a large variation in the shape of the channel response across the length of the array. The channel closest to the surface exhibits a relatively strong principal arrival, while as the depth is increased, a strong second, and eventually third reflections emerge.

Suppose that a full-complexity multichannel equalizer is restricted to operate in a configuration with only three of the 20 channels available. Because of the high spatial variability of the underwater channel, significantly different performance quality may result depending on the choice of the three channels. On the other hand, preceding the three-channel equalizer by an adaptive combiner which operates on all 20 channels increases the number of coefficients to be computed per iteration only by 20×3. If each of the equalizer branches has 60 taps, which is sufficient for about 60 ms of significant multipath at 500 sps, the increase in computational complexity is the same as if one more channel were added to the full-complexity equalizer. However, while the fourth channel may contain a low-quality signal, the 20×3 combiner will adaptively form the best 3-channel combination and pass it to the multichannel equalizer. The only condition that needs to be satisfied to achieve such performance is that the receiver parts be optimized jointly.

Considering the example of 500 sps 8-PSK transmission over 48 nautical miles, the performance of a full-complexity 3-channel equalizer ranges from the best-case output SNR of about 16 dB to cases where the three channels chosen contained such low-quality signals that the algorithm was unable to maintain convergence after the training period. Combining both high- and low-quality channels in a jointly optimal

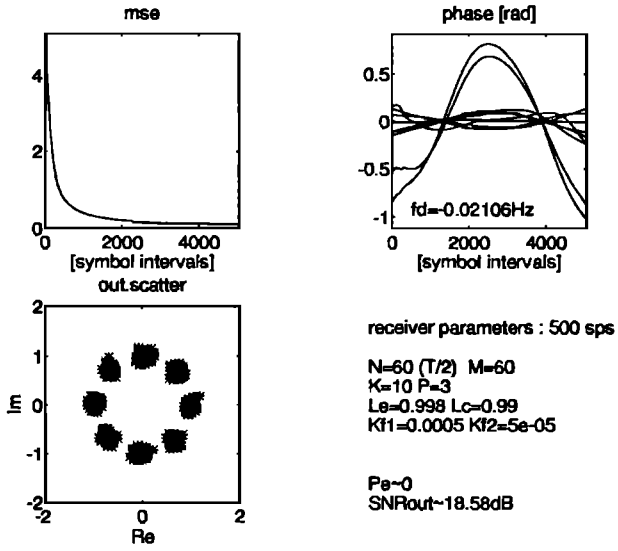

FIG. 9. Receiver performance at 48 nautical miles, 500 sps.

10×3 beamformer and a 3-channel DFE, resulted in the performance shown in Fig. 9. Shown in the figure are the estimated MSE, the carrier phases in all ten channels, and the output scatter plot of the estimated data symbols. Receiver parameters are listed in the figure ($L_{c,e}$ denote the forgetting factors of the combiner and the equalizer RLS algorithms, respectively). In this configuration, the reduced-complexity receiver yielded an improvement of 2 dB in the output SNR over the best case 3-channel DFE performance. No errors were detected in a data block of 10 000 symbols. In addition, the receiver performance was insensitive to the choice of the ten input channels among the 20 available channels.

Excellent results were also achieved with 1000-sps signaling. Figure 10 illustrates the performance of a 7×3 combiner and 3-channel equalizer at 2000 bits per second signaling over 48 nautical miles. The results for QPSK are summarized in Fig. 11 which shows receiver performance in several configurations. The output SNR is shown as a func-

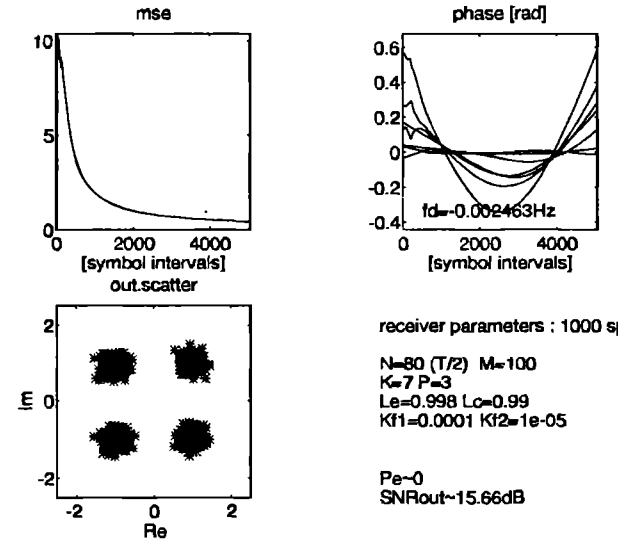

FIG. 10. Receiver performance at 48 nautical miles, 1000 sps.

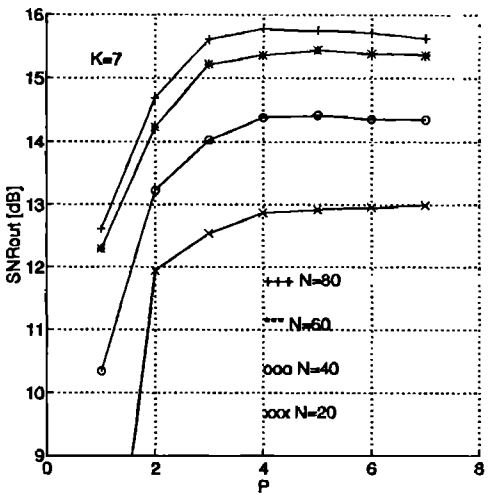

FIG. 11. Output SNR as a function of the reduced number of equalizer channels P.

tion of the reduced number of channels, P, which is varied from $P=1$ to $P=K=7$. The parameter on the curves is the total number of equalizer taps per channel, N. The length of the feedback filter is kept constant, $M=100$. Naturally, performance improves as P increases. However, what is interesting to note is that there exists a form of saturation in performance: Already for $P=3$ the output SNR reaches a value which remains almost constant with further increase in P. While an increase in P from $P=1$ to $P=3$ results in dramatic improvement in performance, changing the number of equalizer channels from 3 to 7 results in the total fluctuation of the output SNR of less than 0.5 dB for all the equalizer lengths examined. This fluctuation is insignificant for the overall receiver performance at the given values of output SNR. The corresponding change in complexity, on the other hand, is considerable: Using a P-channel configuration instead of the "optimal" full-complexity configuration, reduces the total number of filter coefficients by about K/P at large values of N. This brings a significant reduction in complexity when the value of P at which "saturation" is reached is low: at $N=60$, only 200 taps are needed in the 3-channel configuration as opposed to 420 taps of the full-complexity structure. No degradation in performance accompanies this complexity reduction. In fact, careful examination of the output SNR behavior reveals that as N increases, the SNR exhibits a slight degradation after a certain value of P. Such behavior is caused by noise enhancement. Its effect is more pronounced for longer adaptive filters, as illustrated by the fact that only the $N=20$ of all the curves presented does not reach a regime where noise enhancement begins to influence performance. Additional degradation may occur in performance of high-complexity structures on rapidly varying channels when stability constraints of the fast numerically stable RLS[13] must be imposed on the equalizer forgetting factor. This degradation, specific only to certain algorithms, is not included in performance results of Fig. 11. The value of the equalizer forgetting factor was chosen to be $L_e=0.998$ in all of the cases presented.

The results obtained demonstrate several important features of simultaneous reduced-complexity combining and equalization. First, the capability to adaptively choose the best P-channel combination among the K channels available eliminates the strong spatial dependency observed in both the single-channel and the full-complexity multichannel receiver. Second, a multichannel processing gain is obtained over the same-size, full-complexity multichannel receiver, thus demonstrating the capability to additionally exploit spatial diversity of the ocean multipath at no increase in computational cost or noise enhancement. Finally, comparison of the performance of reduced-complexity structures to that of their full-complexity counterparts which operate on all the available channels shows the saturation in the output SNR. Hence, the receiver performs equally well in a configuration that has a small number of equalizer channels.

IV. SUMMARY AND CONCLUSIONS

High-speed UWA communication systems, being inherently broadband due to the large energy absorption at high frequencies, require computationally intensive receiver algorithms for multichannel, spatial and temporal signal processing. The use of large broadband array processors implies problems of noise enhancement and convergence rate tradeoffs in fast transversal filters. In addition to these problems, meeting the computational needs of the receiver algorithm will become a serious problem for multichannel processing in medium and short-range UWA communications where much higher bandwidths than those of the long-range telemetry channels are available.

There is a certain gap, if only in terminology, between approaching the problem of multichannel signal processing from the viewpoint of diversity combining and that of beamforming. With the goal of making large arrays compatible with powerful, but complex time-processing algorithms, we attempted to bridge this gap by examining the role of beamforming in the detection of multipath-corrupted communication signals.

The optimal receivers, nonlinear and linear, consist of an identical combiner, while all the subsequent processing is performed in a single, discrete-time channel. If there exists a relationship between the signals at different sensors, such as in the narrow-band case, the optimal combiner can be identified as a beamformer and a bank of path-matched filters. In contrast to conventional multipath suppression techniques, it is designed to make use of all signal reflections rather than treating them as unwanted interference.

The optimal combiner gives rise to two classes of adaptive implementations. The first class makes no assumptions about the relationship between the received signals, while the second class explicitly uses knowledge of the angles of signal arrivals. The receiver of the second class relies heavily on the assumption that the spatial distribution of signals is known and will be sensitive to any model mismatch. The receiver of the first class, while independent of the existence of any spatial distribution of signals, has a very high computational complexity when a large array is used together with long equalizers.

To compare the approaches considered, a simple condition for equality between the two classes of receivers is ob-

tained. It shows that when the number of sensors is larger than the number of propagation paths, the beamforming interpretation of the optimal combiner offers the possibility of reducing the complexity of a pure diversity combiner, while retaining the same performance. Split beamforming, in which parts of the array are dedicated to beamforming toward individual propagation paths, cannot achieve the performance of a full-matrix beamformer. Both the conventional and the "optimal" beamformer, on the other hand, achieve the same performance as the fully adaptive multichannel equalizer. Hence, proper spatial combining offers the means of reducing the sometimes unacceptable computational complexity of pure diversity combining. For an unknown spatial signal distribution, this is accomplished by jointly optimizing an unconstrained matrix beamformer and a reduced-complexity multichannel equalizer. In practice, such an approach is preferable to the explicit angle of arrival tracking because it does not require accurate initial estimates, nor does it rely on any assumptions such as plane-wave propagation, and therefore eliminates the sensitivity to modeling errors.

A practical receiver proposed uses this type of combining simultaneously with multichannel carrier phase recovery and decision-feedback equalization. Regardless of the specific spatial signal distribution, combining a large number of array signals into a smaller number which are then processed in a multichannel equalizer offers a solution for reducing the receiver complexity without sacrificing the available spatial diversity gain. Joint optimization of the beamformer, the multichannel carrier phase estimator and the DFE provides compatibility of coherent spatial and temporal MMSE combining.

Experimental results demonstrate the excellent performance of the reduced-complexity adaptive combining/equalization algorithm at 50 nautical miles in shallow water with data rates up to 2000 bits per second. Besides providing an additional multichannel processing gain at little or no increase in computational complexity, the receiver overcomes spatial dependency of previous multichannel equalizers without requiring *a priori* knowledge of propagation conditions.

Further potential of reduced-complexity multichannel equalization will become apparent in the case of multiuser signal reception where in addition to multipath recombining, the beamformer will accomplish spatial separation of the desired signal from multiple-access interference.

ACKNOWLEDGMENTS

This work was supported in part by the ARPA Marine Systems Technology Office, Grant No. MDA-972-91-J-1004.

[1] J. Catipovic and L. Freitag, "High data rate acoustic telemetry for moving ROV's in a fading multipath shallow water environment," Proc. 7th International Symposium on Unmanned Untethered Submersible Technologies, 269–303 (1990).

[2] J. Fischer, K. Bennet, S. Reible, J. Cafarella, and I. Yao, "A high rate, underwater acoustic data communications transceiver," in *Proc. Oceans'92*, Newport, RI (IEEE, New York, 1992), pp. 571–576.

[3] M. Stojanovic, J. Catipovic, and J. Proakis, "Phase coherent digital communications for underwater acoustic communications," IEEE J. Oceanic Eng. **OE-19**, 100–111 (1994).

[4] A. Quazi and W. Konrad, "Underwater acoustic communications," IEEE Commun. Mag. **20**, 24–29 (1982).

[5] R. Coates, "Underwater acoustic communications," in *Proc. Oceans'93*, Victoria, Canada (IEEE, New York, 1993), III-420-425.

[6] A. Baggaroer, "Acoustic telemetry—an overview," J. Oceanic Eng. **OE-9**, 229–235 (1984).

[7] L. Wu and A. Zielinski, "Multipath rejection using narrow beam acoustic link," in *Proc. Oceans '88*, Baltimore, MD (IEEE, New York, 1988), pp. 287–290.

[8] J. Catipovic and L. Freitag, "Spatial diversity processing for underwater acoustic telemetry," IEEE J. Oceanic Eng. **OE-15**, 205–216 (1991).

[9] M. Stojanovic, J. Catipovic, and J. Proakis, "Adaptive multichannel combining and equalization for underwater acoustic communications," J. Acoust. Soc. Am. **94**, 1621–1631 (1993).

[10] Q. Wen and J. Ritcey, "Spatial equalization for underwater acoustic communications," in Proc. 26th Asilomar Conference on Signals, Systems and Computers, 1132–1136 (1992).

[11] R. Gooch and B. Sublett, "Joint spatial and temporal equalization in a decision-directed adaptive antenna system," in Proc. 22nd Asilomar Conference on Signals, Systems and Computers, 255–259 (1988).

[12] O. Hinton, G. Howe, and A. Adams, "An adaptive, high bit rate, sub-sea communications system," *Proceedings of the European Conference on Underwater Acoustics*, Brussels, Belgium, edited by M. Weydert (Elsevier Applied Science, Amsterdam, 1992), pp. 75–79.

[13] D. Slock and T. Kailath, "Numerically stable fast transversal filters for recursive least squares adaptive filtering," IEEE Trans. Signal Process. **SP-39**, 92–114 (1991).

[14] P. Bragard and G. Jourdain, "A fast self-optimized LMS algorithm for nonstationary identification. Application to underwater equalization," in Proc. ICASSP'90, 1425–1428 (1990).

[15] R. Monzingo and T. Miller, *Introduction to Adaptive Arrays* (Wiley, New York, 1980).

[16] P. Monsen, "Theoretical and measured performance of a DFE modem on a fading multipath channel," IEEE Trans. Commun. **COM-25**, 1144–1153 (1977).

[17] P. Balaban and J. Salz, "Optimum diversity combining and qualization in digital data transmission with applications to cellular mobile radio," IEEE Trans. Commun. **COM-40**, 885–895 (1992).

[18] D. Chapman, "Partial adaptivity for the large array," IEEE Trans. Antenna Propag. **AP-24**, 685–696 (1976).